Level scheme of ^{101}Zr and structure of the $N = 61$ Sr, Zr, and Mo isotones

G. Lhersonneau,* H. Gabelmann,† M. Liang,‡ B. Pfeiffer, and K.-L. Kratz
Institut für Kernchemie, Universität Mainz, D-55099 Mainz, Germany

H. Ohm
Institut für Kernphysik, Forschungszentrum Jülich, D-52405 Jülich, Germany

and the ISOLDE Collaboration
CERN, CH-1211 Genève 23, Switzerland
(Received 11 October 1994)

The neutron-rich nucleus $^{101}_{40}Zr_{61}$ has been studied at the isotope separator ISOLDE via the β decay of ^{101}Y. A detailed level scheme has been obtained from γ-ray singles, γ-γ-t and β-γ-t coincidence measurements. The level structure of ^{101}Zr is similar to that of its isotone ^{103}Mo showing that, in contrast to their Sr neighbors, the Zr isotopes do not reach maximum of deformation immediately at its onset. This result is rather well reproduced by particle-rotor coupling calculations. A level systematics for the deformed $N = 61$ isotones of $_{38}$Sr, $_{40}$Zr, and $_{42}$Mo allows the assignment of Nilsson configurations to several rotational bands.

PACS number(s): 27.60.+j, 23.20.Lv

I. INTRODUCTION

The neutron-rich $_{40}$Zr isotopes are especially interesting for nuclear-structure studies in the $A \simeq 100$ region. It is well known that the onset of ground-state deformation between neutron numbers $N = 58$ and $N = 60$ is dramatic when viewed in terms of the 2^+_1 energies, dropping from 1223 keV in ^{98}Zr to 213 keV in ^{100}Zr [1]. More recent detailed spectroscopic investigations have shown that the $N = 56$ nucleus ^{96}Zr has a semimagic character [2], whereas ^{98}Zr exhibits shape coexistence [3,4], and ^{100}Zr is with $\beta_q = 0.32(1)$ highly deformed in its ground state [5–7]. For the $N = 62$ isotope ^{102}Zr [8], a further increase of deformation to $\beta_q = 0.37(2)$ has been obtained from earlier lifetime measurements [9]. A systematics of moments of inertia versus ground-state deformations was presented briefly in [3]. It revealed a strong linear correlation, apparently without mass dependence, for ^{100}Zr and ^{102}Zr, as well as for their immediate neighboring $_{38}$Sr and $_{42}$Mo isotones. Accordingly, the identical bands observed in Sr isotopes result from the insensitivity of the moments of inertia to the addition of a few valence nucleons outside a ^{98}Sr core, in agreement with the conclusions of Mach *et al.* [10], and the phenomenon of saturation of deformation in the ^{98,99,100,101}Sr isotopes. As discussed by the TRISTAN group [6,11,12], the closely lying 0^+ states, in both $N = 60$ isotones ^{98}Sr and ^{100}Zr, are strongly mixed. Even in the $N = 58$ nucleus ^{98}Zr, where the separation between the spherical 0^+_1 ground state and the deformed 0^+_3 excited state is about 1.5 MeV, the large ρ^2 value [4] can only be accounted for by large mixing. The mixing between configurations with different shapes has been shown in [6,11] to perturb transition probabilities and level energies. In particular, the deformed 0^+_1 ground states are pushed down by their interaction with the 0^+_2 states. Presumably, this prevents the ground-state bands in ^{98}Sr and ^{100}Sr [13] from being identical down to spin zero.

The picture of shape coexistence presented in [4] has shed new light on the phenomenon of deformation in the $A \simeq 100$ region. With the increasing occupancy of the $\nu g_{7/2}$ and $\nu h_{11/2}$ orbitals, resulting in a larger interaction with the $\pi g_{9/2}$ orbital, a fast but steady lowering of a strongly deformed minimum ($\beta \simeq 0.3 - 0.4$) of the potential-energy surface is observed. This minimum is at about 1.5 MeV excitation energy in the $N = 58$ Sr and Zr isotones, drops to about 0.6 MeV in the $N = 59$ isotones and becomes the strongly deformed ground state of the $N = 60$ isotones, below the spherical minimum at about 0.3 MeV (see, e.g., Fig. 8 in [4]).

In contrast to the even-even nuclides, until recently detailed information on odd-neutron Zr isotopes was scarce. From decay studies at the separators OSTIS and JOSEF [14], shape coexistence could be identified in $^{99}Zr_{59}$ [4]. For the nucleus $^{101}Zr_{61}$, the first odd-neutron Zr isotope in the deformed region, the ground-state band and an excited rotational band have first been reported by Wohn *et al.* [15]. These bands have recently been extended to higher spins in a prompt fission study by Hotchkis *et al.* [16]. The deformation of ^{101}Zr was measured at the separator JOSEF by Ohm *et al.* [17]. However, their value of $\beta = 0.32(6)$ does not allow a conclusion whether deformation increases smoothly with neutron number up to the neutron midshell at $N = 66$, or whether it saturates

*Now at Department of Physics, University of Jyväskylä, P.O.B. 35, FIN-40351, Jyväskylä, Finland.
†Now at KSM-Analytic, D-55129 Mainz, Germany.
‡Now at Department of Physics, University of Edingburgh, Edingburgh EH9 3JZ, UK.

at a value comparable to that of ^{102}Zr. This question is of interest in the light of our recent data for the $_{38}$Sr isotopes with the same neutron numbers [13] which do show saturation of strong ground-state deformation ($\beta \simeq 0.40$) already at its onset at $N = 60$.

Thus, the present study is aimed at clarifying the experimental situation in order to provide a basis for a, still missing, microscopic interpretation. In addition, ^{101}Zr is the link between the strongly deformed $N = 61$ nucleus ^{99}Sr ($\beta = 0.41(3)$ [18,19]) and its, somewhat less, deformed isotone ^{103}Mo ($\beta_q = 0.34(2)$ [20]). The detailed knowledge of the ^{101}Zr level scheme will thus allow a systematic study of neutron levels versus deformation in the $N = 61$ Sr, Zr and Mo isotones.

II. EXPERIMENTAL SETUP AND DATA ANALYSIS

A. Production method

The isotope ^{101}Zr was obtained as a β-decay product of mass separated ^{101}Sr at the CERN-ISOLDE facility. A 12 g/cm^2 uranium-carbide target was exposed to the 600 MeV proton beam from the Synchrocyclotron. After fast diffusion from the target, the Sr isotopes were ionized by a surface-ionization source and mass separated. About 2000 Sr^+ ions were produced per s. The ion beam was collected on an aluminized Mylar tape, viewed by various detectors. The tape transport made it possible to keep the level of long-lived activities low. Collection times of about 1 h were chosen in order to obtain saturation activities for the short-lived daughter products in mass chain $A = 101$. With this, ground-state β feedings could be measured by the filiation method.

B. Detector setup

The β and γ decays were studied by conventional spectroscopic techniques. Gamma-ray singles spectra were recorded with a Ge(HP) detector with 20% efficiency and 1.8 keV FWHM resolution at 1.33 MeV. In order to reduce the room background the Ge detector was gated by the time signal from a thin (3 mm) plastic scintillator triggered by β particles, with a time window of about 0.8 μs. This detector covered the energy range from 12 keV to 4.1 MeV. Three parameter γ-γ-time coincidences were recorded with the Ge(HP) detector and a small planar Ge detector (area 4.9 cm^2, thickness 1.3 cm) having a resolution of 0.55 keV at 122 keV. This detector covered the energy range from 6 keV to 810 keV. From the intensity ratio of the K_α x rays to γ rays in selected gates, conversion coefficients could be obtained by the fluorescence method. For the determination of level lifetimes, coincidences between β particles and γ rays measured with the small Ge detector were recorded as two parameter γ-time events. The time signal from the small Ge detector was split and fed into two constant fraction discriminators in the way described in [21]. In this way, one branch was optimized for high coincidence efficiency at the energy of the x rays ($\simeq$ 15 keV) and the other one for timing. The timing resolution was 5.3 ns at 122 keV.

During a period of about 40 h, a total of 1.9×10^6 γ-γ coincidence events were recorded, mainly corresponding to decays in the $A = 101$ chain. Data acquisition was performed with the GOOSY on-line system at ISOLDE. Coincidence events were recorded in list mode and stored on magnetic tape for off-line processing.

C. Data analysis

The various coincidence events were sorted off line in order to build coincidence matrices. A total of 131 gates in the energy range of 6 keV to 782 keV were set on peaks belonging to the projection onto the small Ge detector. These gates were used for both the analysis of the β-γ-t events for lifetime determinations and the analysis of the γ-γ coincidences. Additionally, for a crosscheck of the γ-γ matrix, 258 gates were set on peaks from the projection onto the large Ge detector in the 43 keV to 2693 keV energy range. Corrections for Compton background contributions were made using windows on both sides of the peak gates, according to the procedure described in [22]. Because of the low coincidence rate of about 10 counts/s it was not necessary to correct for random coincidences by setting a separate gate on the time peak. Nevertheless, their intensities were estimated from the peak areas of the 276.1 keV (^{101}Mo) or the 306.8 keV (^{101}Ru) γ lines which were dominant in the singles spectra but showed only very weak γ-γ coincidences.

Energy and efficiency calibrations were made using activities present as β-decay products of ^{101}Sr. In particular, the recent data on the level scheme of ^{101}Y [23] were used in the range 79.7 keV to 2693.8 keV. Other reference energies could be taken from the crystal spectrometer data on ^{101}Mo [24], from the Table of Isotopes [1] and the relevant Nuclear Data Sheets [25]. Transition energies and intensities were deduced as average values from the analysis of the singles spectra and of selected gates on both detectors in the coincidence set up.

For the determination of conversion coefficients by the fluorescence method, the calibration of the on-line coincidence efficiency is quite critical. The efficiency in the energy region of the x rays was measured using the 13.5 keV $M1$ transition in ^{101}Mo [24] and K_α x-rays of a number of transitions whose conversions are known. These lines consisted of the 128.3 keV transition in ^{101}Y ($\alpha_K = 0.091$ was deduced from the analysis of the ground-state band by [23]), the 43.5 keV transition in ^{101}Mo ($\alpha_K = 8.7(8)$ [24]), the 127.2 keV line in ^{101}Ru [1] and finally, the $E2$ transitions of 118.6 keV (^{100}Zr) and 159.5 keV (^{100}Mo) [26], which are populated via β-delayed neutron emission. Theoretical conversion coefficients were calculated with a simple interpolation code [27].

The time spectra from the β-γ coincidences were analysed by the centroid-shift method. The energy dependence of the position of the prompt reference peak was determined with a ^{152}Eu standard source, recorded before and after the on-line measurement, covering a range of γ energies from 40 keV to 778 keV. The energy de-

pendence of the prompt curve was obtained by a fit of the centroids versus the reciprocal of the γ-ray energies. The limit of the accuracy was about 0.1 ns for γ-ray energies above 120 keV. At lower energies the uncertainties rapidly increased due to the scarcity of calibration points. The accuracy of the prompt curve was estimated to 0.6 ns at 66 keV, which was the lowest-energy on-line reference point [10].

III. RESULTS

A. Level scheme

All previously reported transitions [17] could be confirmed. However, with increasing energy, the γ-ray energies become systematically lower and their intensities higher than quoted in the above paper. The present level scheme includes 22 levels with 61 transitions. Most levels which were previously based on a single coincidence are now firmly established. The transitions are listed in Table I, together with their coincident lines. Several ground-state transitions do not show up in the γ gates. Some of them are masked by contaminants in the singles spectra. Therefore, the determination of their intensities deserves special care. This applies in particular for the ^{101}Zr γ line at 759.5 keV (+ 759.7 keV in ^{101}Nb), the doublet at 1297.7 and 1297.9 keV (+ 1297.6 keV in ^{101}Y) and for the 1529.9 keV line (+ 1530.3 keV in ^{101}Tc). In view of the implications on the understanding of the level scheme, the ground-state transition of 759.5 keV needs to be discussed in some detail. The level at 759.5 keV was established previously by the 98.2 − 661.4 keV coincidence [17]. However, the corresponding ground-state transition was not reported. It might have been masked by the 759.7 keV transition in ^{101}Nb [28]. We have deduced its intensity in ^{101}Zr after subtracting the contribution from Nb (about 10% of the total peak area) by using the data of [28] for normalization. The ground-state transition in ^{101}Zr appears to be the third strongest in the level scheme.

The level at 231.9 keV seems to be somewhat more strongly fed than reported in the previous experiment of Ref. [17]. The origin of this additional feeding ($\simeq$ 6 relative γ-intensity units) is not clear. It might indicate in our case the presence of a short-lived isomer which decays to the 231.9 keV level. We also note that, compared to the recent prompt fission study of [16], we have observed some additional weak low-energy transitions which turned out to be crucial for the assignment of excited bands.

The β branching to the ^{101}Zr ground state was deduced from the γ-ray singles spectra by comparing the intensity of the 205.6 keV transition in ^{101}Nb ($I_\gamma = 0.061(15)$ per ^{101}Zr decay [28]) to those of the 98.2, 104.4, 133.7, and 216.7 keV lines in the level scheme of ^{101}Zr. The method assumes that the independent ionization of Zr is negligible, so that the intensity of the 205.6 keV line originates solely from ^{101}Y decay by filiation. In addition, β-delayed neutron emission from ^{101}Zr has to be negligible. Both requirements are well satisfied. Our measurement yielded an absolute γ intensity of 0.30(8) per decay for the 98.2 keV transition. Accordingly, a ground-state β branch of 0.19(21) was deduced.

The level scheme is shown in Figs. 1 and 2. All adopted levels are based on at least one clear coincidence or several weaker coincidences showing up in a consistent pattern. Only six weak lines listed in Table I have not been included in the scheme. logft values are calculated using the β-decay half-life of 0.565(50) s for the ^{101}Y ground state [29] and the Q_β value of 8.54(9) MeV [30]. For some levels, spin and parity assignments can be deduced from the logft values and the γ transition rates. A list of ^{101}Zr levels is given in Table II.

For the first time, conversion coefficients have been determined for the 98.2, 104.4, and 133.7 keV transitions (Table III). The projections relevant for the 98.2 and 104.4 keV lines are shown in Fig. 3. For both lines, the conversion coefficients establish $M1/E2$ multipolarity.

B. Level lifetimes

The centroid positions for the strongest time peaks of the β-γ-t coincidences are plotted in Fig. 4. Four lines in ^{101}Zr show a measurable delay, namely the 98.2 keV and 216.7 keV ground-state transitions and the 104.4 and 223.0 keV γ rays which both deexcite the 321.2 keV level (Table IV). As expected from [17], these delays are due to the lifetime of the 98.2 keV level, but in addition they also imply a measurable lifetime for the level at 321.2 keV. Since there is no clear evidence for further delayed transitions, the contributions from other levels to the experimental centroid shifts have been neglected. The half-lives of the 98.2, 216.7, and 321.2 keV levels have been obtained from a least-squares analysis of the various observed centroid shifts (see Table V).

The deduced value of 0.39(18) ns for the 98.2 keV level overlaps rather poorly with the previous value of $t_{1/2} = 0.9(3)$ ns of Ref. [17]. The reason is not obvious. Our coincidence data do not provide evidence for a contaminating "prompt" transition of about 98 keV, which could account for a smaller experimental centroid shift. It is therefore more probable that the discrepancy results from systematical errors in the respective prompt curves. In the following discussion, we therefore adopt the average value of $t_{1/2}(98) = 0.6(2)$ ns.

For the level at 321.2 keV a half-life of 0.3(1) ns is obtained (Table V). For the subsequent analysis, the partial γ half-life of the intraband transition of 104.4 keV (to the bandhead at 216.7 keV) is the relevant quantity. The correction for internal conversion and competing transitions is discussed in a later section.

In addition, the line at 216.7 keV shows a measurable delay. The 216.8 keV line in ^{101}Mo [24] could be a possible contaminant. However, this line is very weak and the stronger 441.1 keV line which depopulates the same level in ^{101}Mo seems to be prompt. Thus, the delay has to be due to the line in ^{101}Zr.

TABLE I. List of γ rays assigned to the level scheme of ^{101}Zr. Weak coincidences and tentative levels are given within brackets. Levels based on one weak coincidence only are not included in the level scheme. 100 γ-intensity units correspond to a β feeding of 30.2%.

Energy (keV)		γ intensity		Placed from / to		Coincident lines
87.44	(19)[a]	1.3	(4)[b]	408.3	321.2	(104)
89.35	(11)[a]	1.1	(5)[b]	321.2	231.9	(134), (147)
98.21	(6)	100.0	[b]	98.2	0.0	(89), 104, 119, 134, 223, 310, 487, 554, 575, 649, 661, 688, 729, (782), 1300
104.43	(7)	8.0	(4)[b]	321.2	216.7	98, 119, 147, 217, (487)
118.56	(12)[a]	4.8	(5)[b]	216.7	98.2	98, (104)
133.67	(6)	24.3	(17)[b]	231.9	98.2	98, 176, (554)
146.64	(7)	2.5	(3)	467.9	321.2	98, 104, (217), (223)
176.44	(9)	3.0	(3)[b]	408.3	231.9	98, 134, (232)
216.68	(7)	44.7	(31)[b]	216.7	0.0	104, (147), (527)
222.97	(7)	6.1	(5)[b]	321.2	98.2	98, (147)
231.91	(15)	13.4	(14)[b]	231.9	0.0	(176), (554)
236.20	(23)[a]	1.0	(4)	467.9	231.9	134
251.18	(24)[a]	0.9	(3)	467.9	216.7	217
309.98	(12)	2.6	(3)	408.3	98.2	98
377.49	(22)[a]	0.8	(3)	845.3	467.9	(104), (147), (251)
378.07	(69)[a]	0.5	(3)	786.5	408.3	(134)
422.99	(70)[a]	0.6	(3)	744.0	321.2	(104)
487.44	(19)	3.6	(5)	808.5	321.2	98, 104, (217), (223)
494.22	(26)[a]	1.2	(5)	902.6	408.3	(134), (232)
524.02	(37)	0.9	(4)	845.3	321.2	(104), (217)
527.32	(12)	6.5	(15)	744.0	216.7	(118), 217
551.65	(27)[a]	1.2	(6)	(783.5	231.9)	98, (134)
554.92	(14)	6.1	(12)	786.5	231.9	98, 134, (232)
571.14	(59)	1.2	(6)	786.5	216.7	(217)
575.47	(18)	5.0	(7)	673.5	98.2	98
577.21	(46)[a]	1.2	(5)	808.5	231.9	(134)
592.05	(27)[a]	2.4	(8)	808.5	216.7	(217)
596.40	(41)[a]	0.9	(5)	827.8	231.9	(98)
611.93	(28)	1.6	(3)	(710.1	98.2)	(98)
624.27	(26)	1.2	(3)	(722.5	98.2)	(98)
645.88	(47)[a]	0.9	(4)	744.0	98.2	(98)
648.59	(16)	8.1	(14)	880.4	231.9	98, 134, (232)
661.39	(12)	14.4	(11)	759.5	98.2	98
670.67	(24)	1.4	(5)	902.6	931.9	(98), (134)
673.21	(28)	4.5	(23)	673.5	0.0	
688.40	(17)	6.2	(8)	786.5	98.2	98
710.06	(55)[a]	0.6	(4)	808.5	98.2	(98)
727.34	(46)	1.5	(6)	958.9	231.9	(98), (134)
729.57	(16)	6.2	(7)	827.8	98.2	98
744.02	(14)	2.2	(5)	744.0	0.0	
746.70	(56)	1.4	(4)	845.3	98.2	(98)
759.45	(7)	30.2	(26)	759.5	0.0	
782.15	(38)[a]	1.4	(5)	880.4	98.2	(98)
786.53	(31)	1.6	(5)	786.5	0.0	
804.51	(47)	1.1	(5)	902.6	98.2	(98)
808.29	(15)[c]	2.2	(6)	808.5	0.0	
827.77	(13)	2.6	(6)	827.8	0.0	
846.67	(33)	1.5	(4)	(944.9	98.2)	(98)
855.84	(32)[a]	1.5	(5)	(954.2	98.2)	(98)
860.77	(68)	1.1	(5)	958.9	98.2	(98)
880.36	(13)	7.8	(11)	880.4	0.0	
940.22	(31)[a]	2.7	(8)	1038.4	98.2	98
954.36	(33)[c]	1.0	(5)	(954.2	0.0)	
958.63	(34)[c]	1.4	(8)	958.9	0.0	
1081.33	(62)[a]	1.7	(8)	1297.9	216.7	(217)
1166.97	(26)	4.6	(7)	1398.6	231.9	(98), 134

TABLE I. *(Continued).*

Energy (keV)		γ intensity		Placed from / to		Coincident lines
1248.06	(44)[a]	1.5	(5)	(1346.3	98.2)	(98)
1297.72	(42)	5.1	(16)	1529.9	231.9	(98), 134
1297.89	(11)	5.9	(38)	1297.9	0.0	
1300.26	(17)	29.7	(23)	1398.6	98.2	98
1398.60	(20)	5.8	(12)	1398.6	0.0	(98)
1432.83	(87)	1.5	(6)	1529.9	98.2	(98)
1529.95	(15)	4.5	(7)	1529.9	0.0	
1925.51	(39)[a]	4.9	(11)	2023.2	98.2	(98)
1984.69	(52)	3.0	(6)	2082.9	98.2	(98)
2023.06	(17)	11.3	(10)	2023.2	0.0	
2082.82	(45)[c]	1.3	(5)	2082.9	0.0	

[a]Line seen only in coincidences, or for which the peak in the singles spectra was masked by contaminants.
[b]Conversion of this line has been taken into account when computing intensity balances.
[c]Line not seen in the projection of coincidence events.

IV. SPIN AND PARITY ASSIGNMENTS

A. The ground-state $K^\pi = 3/2^+$ band

The ground state and the 98.2, 231.9, and 408.3 keV levels were identified by Ohm *et al.*, Ref. [17], as members of a rotational band with $K = 3/2$. Even parity for the ground state of ^{101}Zr is well established by the allowed character of the β decay to the [422]5/2$^+$ ^{101}Nb ground state [28]. This band has recently been extended up to spin 17/2 in the prompt fission study by Hotchkis *et al.* [16]. There is no clear evidence that further band members with $I \geq 11/2$ are observed in the β decay of ^{101}Y ($I^\pi = 5/2^+$) [23] to ^{101}Zr. Guided by the data of [16], the marginal coincidences at 201.8(5) keV [$I_\gamma = 0.2(1)$] and 378.6(5) keV [$I_\gamma = 0.9(6)$] in the 176.4 and 133.7 keV gates, respectively, might be an indication of a very weak population of the 11/2 band member. Although, as was already mentioned, we obtain a stronger feeding of the 231.9 keV level than in the previous experiment at JOSEF [17], the intensity ratios of the crossover to stopover transitions of 0.55(7) (this work) and 0.63(10) [17], do agree within their uncertainties. This fact is important for the band analysis since this ratio determines the $|(g_K\text{-}g_R)/Q_0|$ band parameter.

The new information for this band includes the measurement of the K-conversion coefficient of the 98.2 keV transition (Table III). The $\delta(E2/M1)$ mixing ratio deduced from the conversion coefficient α_K compares well with the one extracted from the band analysis (Tables VI and VII), following the procedure described in [31]. The deformation parameter β deduced from the mean value of the lifetime measurements in this work and by Ohm *et al.* [17], i.e., $t_{1/2}(98) = 0.6(2)$ ns, is $\beta = 0.37(7)$. Unfortunately, the large uncertainty does not allow a conclusion about a further increase or a saturation of deformation when going from ^{100}Zr ($\beta = 0.34(1)$ [5]) to ^{101}Zr. However, it will be shown later that a more accurate value for ^{101}Zr can be obtained indirectly from level systematics of the $N = 61$ isotones.

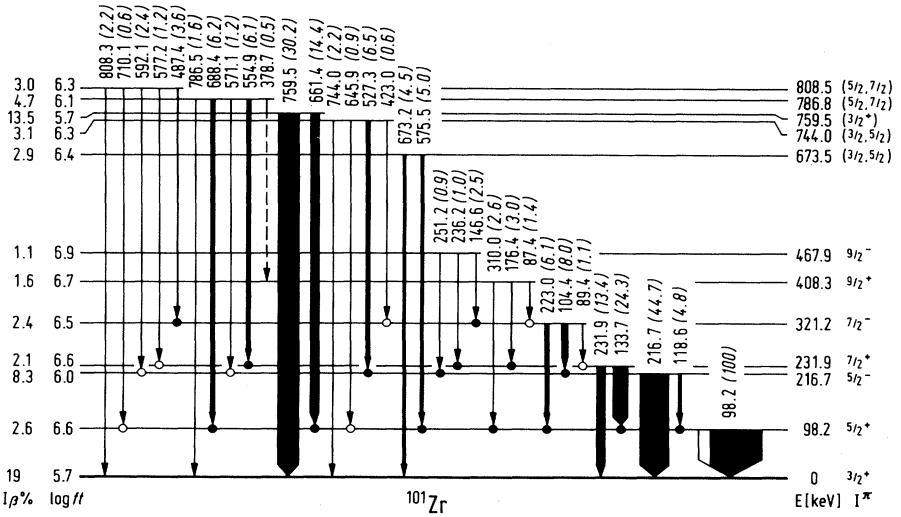

FIG. 1. Low-energy part of the decay scheme of ^{101}Y into ^{101}Zr. Full (open) circles represent clear (weak) coincidences. Dashed lines indicate low-intensity transitions which have not been seen as coincidences, but whose energies fit well between the levels. These transitions were not included in the calculation of the intensity balances. Level spin and parity assignments are indicated if less than 3 alternatives.

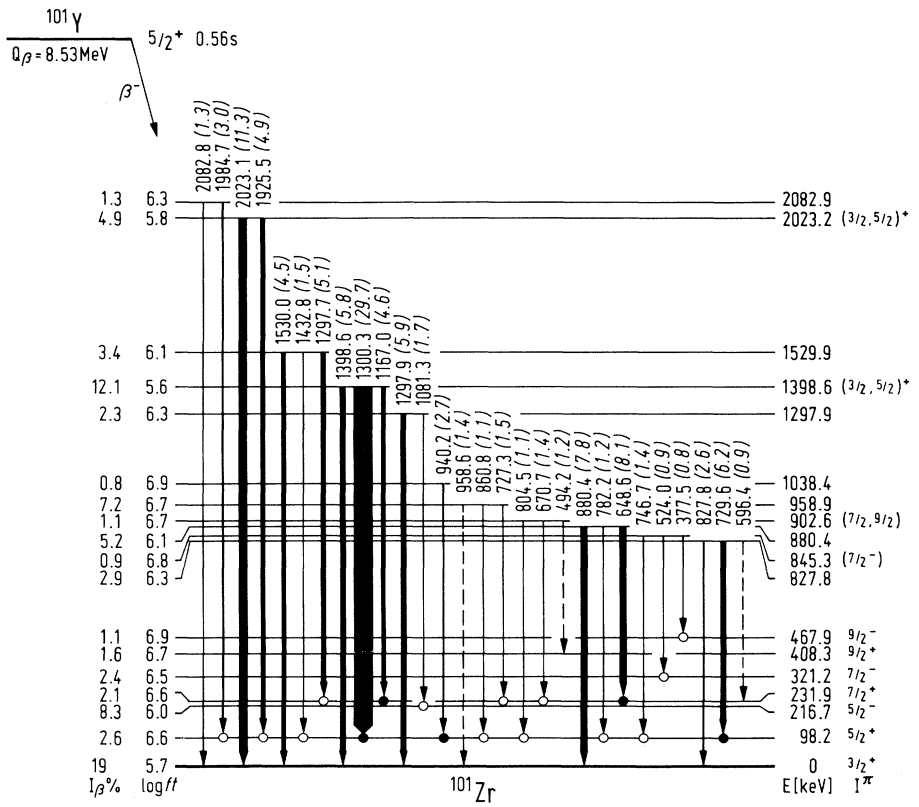

FIG. 2. High-energy part of the decay scheme of ^{101}Y into ^{101}Zr. For legend, see Fig. 1.

B. The first excited $K^\pi = 5/2^-$ band

The levels at 216.7, 321.2, and 467.9 keV (see Fig. 1) form an excited band. Since the rotational spacings are close to those of the $K = 3/2$ ground-state band, Wohn *et al.* [15] suggested a $K = 3/2$ value also for this excited band. More recently, this band has been extended up to spin 19/2 [16]. However, based on the Alaga γ-branching rules for transitions between rotational states these authors favor a $K = 5/2$ assignment. In both reports [15,16], odd parity has been assumed for the excited band according to Nilsson-model considerations and Coriolis mixing. Indeed, the β feeding of the 216.7 keV bandhead ($\log ft = 6.0$) and of the next rotational level at 321.2 keV ($\log ft = 6.5$) are consistent with first-forbidden transitions. Moreover, the half-life of 0.3 ns for the 216.7 keV bandhead (Table V) corresponds to a hindrance of about 10^4 relative to the Weisskopf estimate for an $E1$ transition. This is a very reasonable hindrance factor. The weak interband transition at 87.4 keV from the $9/2^+$ level of the $K = 3/2$ ground-state band to the $I = K+1$ level of the excited band, which was not observed in the mentioned previous studies [15,16], competes successfully with the intraband transitions at 176.4 keV ($M1$; $9/2^+ \rightarrow 7/2^+$) and 310.0 keV ($E2$; $9/2^+ \rightarrow 5/2^+$). A direct measurement of the multipolarity of the 87.4 keV transition was not possible due to the limited counting statistics. Nevertheless, since the lifetime measurements exclude that the transition of 87.4 keV has $M2$ character, $K = 3/2$ can be definitely excluded for the sideband, thus leaving $K = 5/2$ (implying $E1$ multipolarity for the 87.4 keV transition) as the only possibility.

In addition, for the first time the conversion coefficient for the intraband $K+1 \rightarrow K$ 104.4 keV transition and the half-life of the $K+1$ level have been measured (see Tables III and V). The conversion coefficients α and α_K for this transition establish its multipolarity as $M1/E2$, with $|\delta| \simeq 0.4$. The γ branching of 0.58(3) is deduced taking into account the competing $E1$ transitions at 89.4 keV and 233.0 keV and the conversion of the 104.4 keV line itself. This yields a partial γ-half-life of 0.47(23) ns for the 104.4 keV transition (Table VI). Although the uncertainty is large, the deduced deformation parameter (Table VII) confirms the large deformation of the nucleus ^{101}Zr.

C. Evidence for further band structure

The level at 759.5 keV is one of the most strongly populated ones. The $\log ft$ value of 5.7 indicates allowed β feeding and, accordingly, even parity of the 759.5 keV level. Moreover, transitions to the $3/2^+$ and $5/2^+$ members of the ground-state band are observed, but branchings to the next $7/2^+$ member level or to levels of the $5/2^-$ band are below a limit of about one γ-intensity unit. Thus, a $I^\pi = 3/2^+$ assignment is most probable.

TABLE II. List of ^{101}Zr levels populated in the β decay of ^{101}Y. For computing logft values, $T_{1/2}(^{101}Y)$ = 0.565 s [29] and the Q_β value of 8.54 MeV [30] have been used. Spin and parity assignments without brackets refer to levels in the $3/2^+$ ground-state and $5/2^-$ first excited bands. Assignments in brackets are based on a systematics of levels with similar decay patterns and a comparison with the trend of Nilsson levels versus deformation.

Energy (keV)		β feeding (%)		logft	I^π, configuration
0.		19.0	(210)	5.7	$3/2^+$, [411]3/2
98.21	(6)	2.2	(24)	6.6	$5/2^+$,
216.70	(6)	8.2	(24)	6.0	$5/2^-$, [532]5/2
231.89	(7)	2.1	(12)	6.6	$7/2^+$
321.17	(6)	2.4	(7)	6.5	$7/2^-$
408.32	(10)	1.6	(5)	6.7	$9/2^+$
467.85	(8)	1.1	(4)	6.9	$9/2^-$
673.53	(22)	2.9	(10)	6.4	$(5/2^+$, [402]5/2)
744.03	(9)	3.1	(10)	6.3	$(3/2^-$, [541]3/2)
759.48	(6)	13.5	(36)	5.7	$(3/2^+$, [422]3/2)
786.74	(12)	4.7	(13)	6.1	$(7/2^+)$
808.49	(12)	3.0	(9)	6.3	$(5/2^-)$
827.80	(10)	2.9	(8)	6.3	
845.25	(19)	0.9	(3)	6.8	$(7/2^-$, [523]7/2)
880.40	(10)	5.2	(15)	6.1	$(5/2^+)$
902.57	(17)	1.1	(4)	6.7	$(9/2^+)$
958.86	(25)	1.2	(5)	6.7	
1038.43	(32)	0.8	(3)	6.8	
1297.89	(11)	2.3	(13)	6.3	
1398.59	(12)	12.1	(33)	5.6	$(3/2^+$, [402]3/2)
1529.94	(15)	3.4	(10)	6.1	
2023.16	(24)	4.9	(14)	5.8	
2082.85	(34)	1.3	(4)	6.3	

If the 759.5 keV level is the head of a $K = 3/2$ band, the Alaga rules would predict a 5% β feeding of the next band $I^\pi = 5/2^+$ member. The 880.4 keV level is a possible candidate for such a level. This interpretation is consistent with the level systematics shown Fig. 5 and discussed in the next section.

The level at 744.0 keV decays not only to the ground-state band but also with a strong branch to the $5/2^-$ bandhead at 216.7 keV (see Fig. 1). This peculiar decay pattern favors odd parity, in which case $I^\pi = 7/2^-$ can be excluded from the observation of a transition to the $3/2^+$ ground state. Another level with similar character is the one at 808.5 keV, which has branches to the $5/2^-$ and $7/2^-$ levels, and also a decay to the ground state. If the parity of the 808.5 keV level is odd, the only possible assignment is $I^\pi = 5/2^-$. In addition, the level at 845.3 keV has strong branchings to the $K = 5/2^-$ band, however only to its $7/2^-$ and $9/2^-$ members (see Fig.

TABLE III. Conversion coefficients.

Energy (keV)	Experimental α_K or α		Theoretical $\alpha_K(M1)$	Theoretical $\alpha_K(E2)$	Mixing ratio $\lvert\delta(E2/M1)\rvert$
98.2	0.24	(6)[a]	0.19	0.98	0.3^{+2}_{-3}
104.4	0.38	(20)[b]	0.19	0.95	0.6^{+5}_{-6}
	0.25	(10)[c]	0.16	0.79	0.4^{+3}_{-4}
					0.4^{+2}_{-4}[d]
133.7	0.00	(14)[e]	0.095	0.36	0.0^{+5}_{-0}

[a] α_K from the intensity ratio $I(K_\alpha)/I_\gamma(98)$, averaged over the gates on the 134, 223, 310, 661, 688, 575, and 1300 keV transitions.

[b] Average α from the intensity balance $I_{tot}(104) = I_{tot}(119)+I_{tot}(217)$ in the projections gated by the 147 and 487 keV transitions. The 119 and 217 keV transitions are assumed $E1$ multipolarity.

[c] α_K from the ratio $I(K_\alpha)/I_\gamma(104)$ in the 217 keV gate. The weak contribution from the 147 keV line to the K_α peak ($\simeq$5%) was estimated using its δ value deduced from the band analysis (Table VII).

[d] Average from [b] and [c].

[e] Average α from the intensity balance $I_{tot}(98) = I_{tot}(134)$ in the projections gated by the transitions at 176, 555, 649, and 1167 keV.

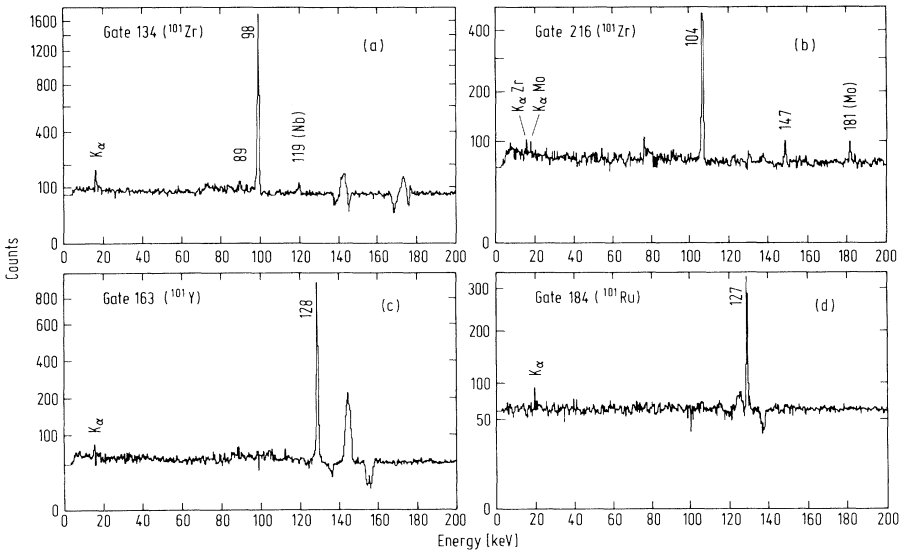

FIG. 3. Coincidence spectra with selected gates showing the data relevant for the determination of the conversion coefficients α_K of the 98.2 [1] and 104.4 keV [2] transitions. Spectra with the projected 128.3 keV (^{101}Y) [3] and 127.2 keV (^{101}Ru) [4] lines and their accompanying x rays are shown for reference.

2). This suggests odd parity and a rather high spin. The branch to the $5/2^+$ member of the ground-state band, however, excludes a $9/2^-$ assignment. Thus, the 845.3 keV level is a good candidate for $I^\pi = 7/2^-$. Summarizing, it is tempting to assume that the levels at 744.0, 808.5, and 845.3 keV are the bandhead and the lowest members of a $K^\pi = 3/2^-$ band.

Another set of selected levels shows decay patterns with branchings to the ground-state band. The level at 673.5 keV is the lowest of the newly identified states (see Fig. 1). The γ decays to the $3/2^+$ and $5/2^+$ levels of the ground-state band with similar strengths and the logft value of 6.4 indicate a low spin $I = (3/2, 5/2)$. The next member of a possible band built on the 673.5 keV level could be the level at 786.7 keV. It decays with strong branches to the $5/2^+$ and $7/2^+$ members of the ground-state band and has a possible decay to the $9/2^+$ level. Thus, its most probable spin is $I = (5/2, 7/2)$. The ground-state transition excludes odd parity if $I = 7/2$. The logft value of 6.1, indeed, seems to favor even parity. The third band member could be the 902.5 keV level. This state also decays to the $5/2^+$ and $7/2^+$ members of the ground-state band and possibly to the $9/2^+$ level, but a transition to the $3/2^+$ ground state is not observed. This is consistent with $I = (7/2, 9/2)$. Fitting the energies of the 673.5, 786.7 and 902.5 keV levels, including the first-order term in $I(I+1)$ and the A_{2K} signature term, one obtains inertia parameters of $a = 20.6$ and 15.3 keV for $K = 3/2$ and $5/2$, respectively. Compared to the a values deduced for the ground-state band and the $5/2^-$ side band (Table VII), both choices of K are reasonable. For $K = 5/2$, this band would, however, have to be perturbed as is the low-lying $5/2^-$ side

Further assignments become very tentative. The levels at 827.8 and 958.9 keV could be members of another $K = 3/2$ or $5/2$ band. Both states decay to the ground-state band, the first with its strongest branch to the $5/2^+$ level, the second to the $7/2^+$ level. This could indicate a spin difference of one unit. The energy spacing of 131.1 keV is consistent with $I(827.8) = 5/2$, if the band is

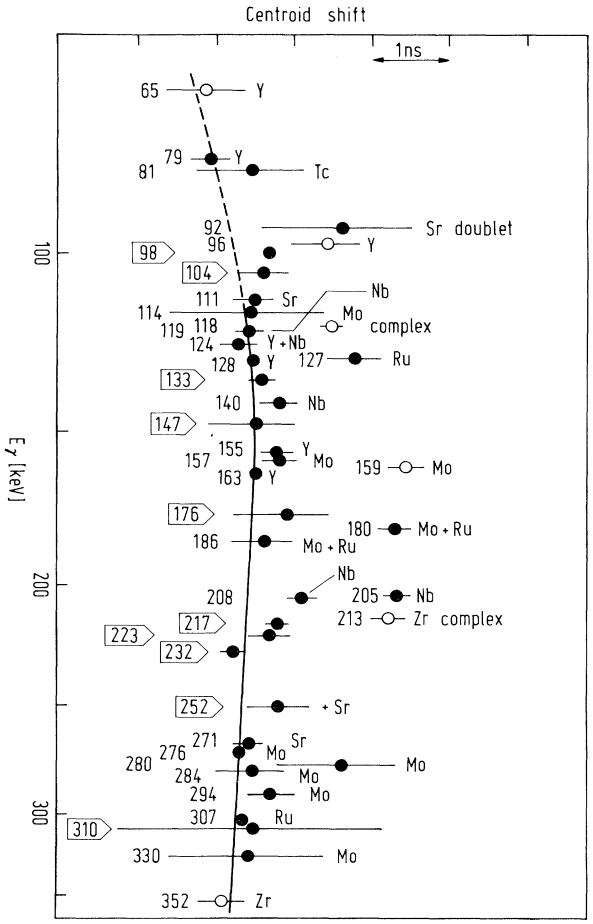

FIG. 4. Centroids of time distributions of on-line β-γ coincidences vs γ-ray energy. Full (open) points belong to isotopes in the mass chain 101 (100). The errors bars of the centroids for the lines at 98, 128, 163, and 307 keV are smaller than the size of the points. Transitions in the level scheme of ^{101}Zr are marked by a frame. The prompt curve is indicated by a solid line where the accuracy is $\simeq$ 0.1 ns, continued by a dashed line at lower energies where the accuracy deteriorates.

TABLE IV. Centroid shifts from β-γ(Ge)-t coincidences. The coefficients for the contributions of the 98, 217, 232, and 321 keV levels are calculated using β and γ intensities from Tables I and II. Other levels do not show a measurable delay. Errors on centroid shifts include statistical errors on the centroids and the systematic error on the prompt reference curve (Fig. 4).

Transition (keV)	Centroid shift (ns)		Origin of the delay
98.2	0.60	(25)	τ_{98} + 0.04$\star\tau_{217}$ + 0.17$\star\tau_{232}$ + 0.06$\star\tau_{321}$
104.4	0.38	(22)	τ_{321}
133.7	0.14	(17)	τ_{232} + 0.04$\star\tau_{321}$
216.7	0.53	(17)	τ_{217} + 0.15$\star\tau_{321}$
223.0	0.45	(36)	τ_{321}
231.9	-0.16	(18)	τ_{232} + 0.04$\star\tau_{321}$

TABLE V. Half-lives extracted from a least-squares analysis of the centroid shifts shown in Table IV and in Ref. [17].

Level (keV)	Half-life (ns) From Table IV		From Ref. [17]	
98.2	0.39	(18)	0.9	(3)
216.7	0.33	(12)		
231.9	-0.02	(9)		
321.2	0.27	(13)		

TABLE VI. Input parameters for the band analysis (Table VII). Half-lives are partial γ-half-lives for intraband transitions.

K	Level (keV)	I^π	Parameters
3/2	98.2	$5/2^+$	$t_{1/2}(98)$ = 0.6(2) ns[a]
	231.9	$7/2^+$	$\frac{I_\gamma(232)}{I_\gamma(134)}$ = 0.59(5)[b]
	408.4	$9/2^+$	$\frac{I_\gamma(310)}{I_\gamma(176)}$ = 0.78(9)[b]
5/2	321.2	$7/2^-$	$t_{1/2}(104)$ = 0.47(23) ns
	467.8	$9/2^-$	$\frac{I_\gamma(251)}{I_\gamma(147)}$ = 0.49(6)[c]

[a]Adopted average from this work and Ref. [17].
[b]Average from this work and Refs. [16,17].
[c]Average from this work and Ref. [16].

TABLE VII. Properties of the $K^\pi = 3/2^+$ and $K^\pi = 5/2^-$ bands, deduced from the input data in Table VI. Reduced transition probabilities $B(M1)$ and $B(E2)$'s are given relative to the single-particle values. $\langle s\rangle$ is calculated using $g_R = 0.5 \star Z/A$ and $g_s = 0.65 \star g_s$(free).

Deduced quantities	K = 3/2 g.s. band		K = 5/2 band	
$a = \hbar^2/(2\star J)$ (keV)	19.4		15.3	
A_{2K} (keV)	0.072		-0.019	
$\lvert(g_K - g_R)/Q_0\rvert$ (b^{-1})	0.164	(24)	0.093	(7)
$\lvert\delta_{K+1\to K}\rvert$	0.24	(4)	0.31	(3)
$\lvert\delta_{K+2\to K+1}\rvert$	0.24	(2)	0.34	(3)
$B(M1, K+1\to K)$ (10^{-2} W.U.)	2.9	(10)	3.0	(15)
$B(E2, K+1\to K)$	160	(68)	241	(121)
Q_0 (b)	3.7	(8)	4.4	(11)
β	0.37	(7)	0.44	(10)
$\langle s_z\rangle$	0.24	(6)	0.21	(10)

unperturbed. Alternatively, the tentative level at 722.5 keV which may result from the 98.2 – 624.3 keV coincidence (see Table I) could be the $K = 3/2$ head of this band. With the three levels at 722.5, 827.8, and 958.9 keV, an inertial parameter of $a = 20.3$ keV is deduced, which compares quite well with the corresponding value for the ground-state band. Unfortunately, the data are too uncertain to make a firm K assignment.

In summary, we have proposed assignments to all levels below 1 MeV. At higher energies, the increasing level density and the limitations of the experiment make further assignments too much unreliable. We only note that the energy spacings of the levels at 1297.9, 1398.6, and 1529.9 keV resemble closely those of the ground-state band, which could indicate a $K = 3/2$ band. Moreover, similarities in the γ-decay patterns can be observed among levels which, however, cannot be grouped within the same band. The levels at 827.8, 1398.6, and 2082.9 keV have their strongest decay to the first excited $5/2^+$ state at 98.2 keV. The level at 1529.9 keV has strong branches to the $3/2^+$ and $7/2^+$ levels of the ground-state band, like the level at 880.4 keV ($5/2^+$). Finally, the decay of the level at 2023.2 keV shows similarities to that of the 759.5 keV level ($3/2^+$).

V. DISCUSSION

A. Deformation of ^{101}Zr

Among the $N = 61$ isotones the nucleus $^{101}_{40}$Zr occupies a position between the strongly deformed $^{99}_{38}$Sr with $\beta = 0.41(3)$ [18,19] and $^{103}_{42}$Mo with $\beta = 0.36(2)$ [20]. For definition of the deformation parameter β, we use the formula $Q_0 = \frac{3}{\sqrt{5\star\pi}} \star Z \star R^2 \star \beta \star (1 + 0.16 \star \beta)$, in order to facilitate comparison with older results. Sometimes, the quantity β_q is used which is, however, practically identical ($\beta_q \simeq \beta - 0.02$) in the $\beta \simeq 0.3$ region. Prior to this work, only a partial level scheme for ^{101}Zr was available from studies at the TRISTAN [15] and JOSEF [17] separators. The new detailed data provide the missing link between the $N = 61$ isotones ^{99}Sr and ^{103}Mo, so that the relative positions of several neutron states can be followed in a systematical way as a function of deformation.

The systematics of selected levels is shown in Fig. 5. Since, within the range of large deformations of $\beta \simeq 0.3 - 0.4$, the energies of most Nilsson orbitals vary smoothly, the deformation of ^{101}Zr can be estimated by an interpolation of the excitation energies of corresponding levels versus deformation parameter β. The result is shown in Fig. 6. Using the first excited $3/2^+$ level, which has been assigned reliably in all three $N = 61$ isotones, ^{99}Sr, ^{101}Zr, and ^{103}Mo, the interpolation yields $\beta_{Zr} \simeq 0.28 \star \beta_{Sr} + 0.72 \star \beta_{Mo}$. Inserting the β values for ^{99}Sr [18,19] of 0.41(3) and for ^{103}Mo [20] of 0.36(2), a deformation parameter of $\beta(\mathrm{Zr}) = 0.37(2)$ is deduced. This value is just the same as was obtained from the average of the lifetime measurements. The validity of the above procedure is supported by the fact that, with the adopted value of $\beta = 0.37$, regular energy trends are obtained also for other levels with similar decay patterns.

Thus, it turns out that ^{101}Zr is more strongly deformed than ^{100}Zr ($\beta = 0.34(1)$ [5]) but probably less than ^{102}Zr ($\beta = 0.39(2)$ [9]). This observation implies that, although both Sr and Zr isotopes show the same qualitative picture of shape coexistence and of fast lowering of the deformed minimum with increasing neutron number [4], only in the Sr isotopes the deformation does reach saturation at its onset. Mach *et al.* [10] have related the saturation of deformation to the maximum occupation of

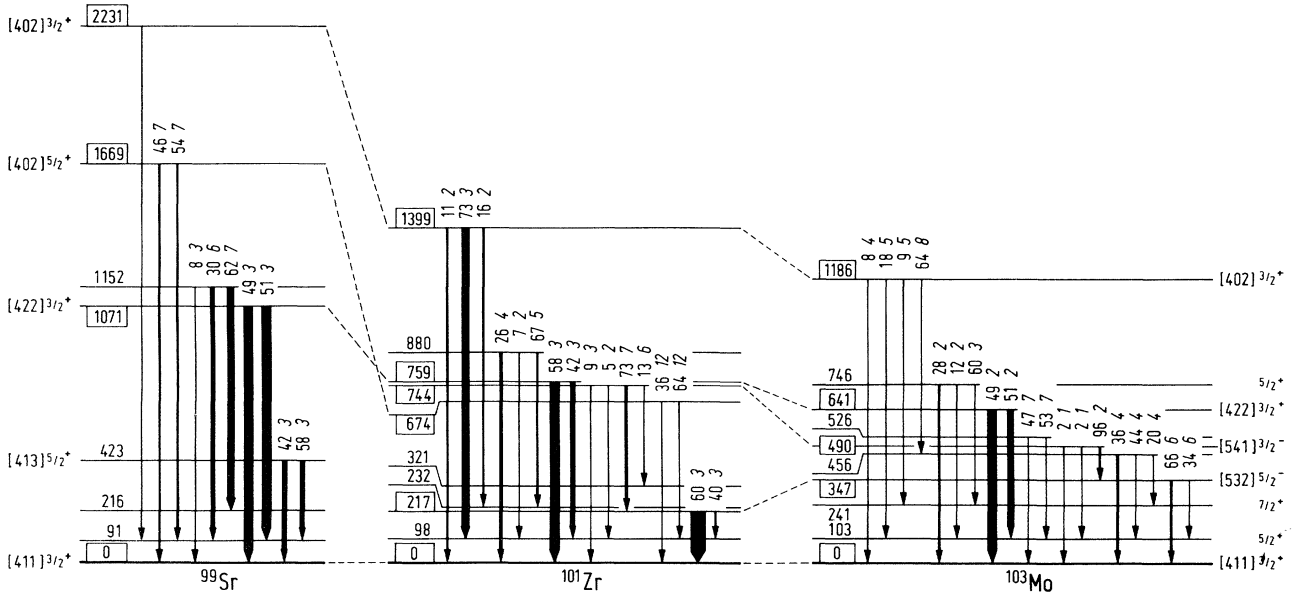

FIG. 5. Comparison of selected levels in the $N = 61$ isotones ^{99}Sr, ^{101}Zr, and ^{103}Mo. The energies of rotational band-heads are set off through boxes. Relative γ-ray intensities are indicated by the thickness of the arrows. Figures are reduced transition probabilities and their uncertainties, normalized to 100 for each level. For discussion, see text.

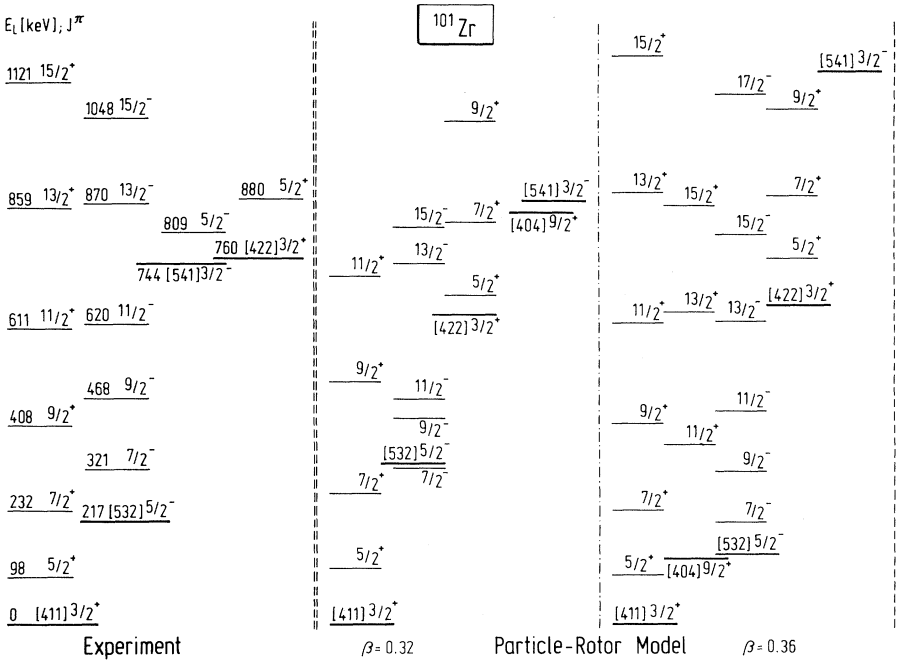

FIG. 6. Comparison of rotational bands in ^{101}Zr with calculations with the particle-rotor coupling model. The agreement is best for $\beta \simeq 0.36$, which is consistent with the measured deformation and with the estimate from the level systematics shown Fig. 7.

down-sloping orbitals near the Fermi surface. However, we note, that in the $N = 63$ isotones ^{101}Sr and ^{105}Mo, both with similar deformations of $\beta \simeq 0.40$, the $3/2^+$ excitation energies above the $5/2^-$ ground states, 271.2 keV [32] and 246.7 keV [16,31,33,34], respectively, are very close. Accordingly, it is unlikely that the occupancies of the neutron orbitals would change dramatically from ^{99}Sr to ^{101}Zr. Thus, there must be another explanation to account for the specific saturation of deformation at its onset in the Sr isotopes, e.g., the integrated proton-neutron interaction [13] in the formalism of [35]. As a matter of fact, in this interpretation, Sr and Zr isotopes differ by the contribution of the last proton pair.

B. Rotational levels

The $\nu[411]3/2$ Nilsson orbital has been assigned to the ground states of the $N = 61$ isotones ^{99}Sr [18], ^{101}Zr [17], and ^{103}Mo [31]. This assignment is confirmed by our analysis in terms of the rotational model (Tables VI and VII). An unexpected feature of the [411]3/2 ground-state bands in these isotones is the linear correlation between moment of inertia and deformation. The values of the moment of inertia are 27.6, 25.5, and 24.8 $\hbar^2 \star \mathrm{MeV}^{-1}$ for ^{99}Sr, ^{101}Zr, and ^{103}Mo, respectively. The trend clearly is opposite to the prediction of the rigid-rotor formula in which the mass enters as $A^{5/3}$ scaling factor. It must be stressed that this phenomenon is not accidental but is observed also for the $N = 60$ and 62 isotones of these elements and is a requisite for the occurrence of identical ground-state bands at low spin in neighboring Sr isotopes [3]. The systematics of moments of inertia will be discussed in more detail in a forthcoming paper [36]. Based on the large gaps between the proton and neutron single-particle levels, a deformed "magic" ^{98}Sr core was proposed by Mach *et al.* [10] to account for g factors in its immediate vicinity. The observed trend of the moments of inertia seems to indicate that even a larger number of valence particles does not affect the ^{98}Sr core.

The excited bandhead at 216.7 keV has been assigned to the $\nu[532]5/2$ orbital [16]. The $5/2^-$ assignment is confirmed by the new low-energy interband transitions. Also the band analysis (Tables VI and VII) is in agreement with the proposed Nilsson configuration. In the slightly less deformed isotone ^{103}Mo the excitation energy of this orbital is expected to lie somewhat higher. Indeed, the level at 346.5 keV in ^{103}Mo shows a decay pattern which is in excellent agreement with that of the level at 216.7 keV in ^{101}Zr (Fig. 5). The same assignment for the ^{103}Mo level was made by Liang *et al.* [20].

In ^{99}Sr, the $5/2^-$ bandhead is not yet identified. Due to the larger deformation, the strongly down-sloping [532]5/2 orbital (of particle character) must come closer to the [411]3/2 ground state. The nonobservation of the $5/2^-$ level in ^{99}Sr, in spite of γ-γ coincidence experiments with high statistics [37], seems to indicate that it lies below or very close above the first excited state $I^\pi = 5/2^+$ at 90.8 keV. In all nuclei observed in the prompt fission study of [16] the $5/2^-$ band is perturbed, showing a compression especially of the low-lying levels. This is also reproduced by calculations with the particle-rotor model (see Sec. IV C).

There are no other levels for which band properties are firmly established from an analysis of γ-ray intraband-branching ratios. However, the energy trend of levels of similar character can be followed in the isotones ^{99}Sr, ^{101}Zr, and ^{103}Mo and compared to the evolution of Nilsson orbitals versus deformation. Following this procedure a number of levels can be associated to Nilsson orbitals (see Fig. 7).

The best established systematics concerns the first excited $3/2^+$ levels. It shows that levels with properties similar to those of the 759.5 keV level exist in both ^{99}Sr and ^{103}Mo (Fig. 5). Thus, the levels at 1071.2 keV (^{99}Sr), 759.5 keV (^{101}Zr), and 641.1 keV (^{103}Mo) have the same nature. The levels in the next set—151.6 keV (^{99}Sr), 880.4 keV (^{101}Zr), and 746.2 keV (^{103}Mo)—also show similar decay properties. These levels are candidates for the $I = K + 1$ band member. We note that, using the Alaga rule for estimating the unknown ground-state β branching in ^{103}Mo, we derive logft values of 4.9 and 5.5 for the proposed 641.1 keV (3/2) and 746.2 keV (5/2) levels, respectively, which indeed supports the postulated even parity. However, Liang *et al.* [20] assign the 692.8 keV level to the $5/2^+$ band member in ^{103}Mo. We believe that this level more likely corresponds to the 786.7 keV state in ^{101}Zr, both having their strongest decay to the $5/2^+$ member of the ground-state band. For the latter our interpretation is different, as discussed below. There is hardly an alternative choice to the ν[422]3/2 orbital for the $3/2^+$ level. Apart from the [411]3/2 ground state, this orbital is the only one with $K^\pi = 3/2^+$ available at low energy. This interpretation is supported by the trend of the levels in the $N = 61$ isotones versus deformation, i.e., the excitation energy of a down-sloping hole orbital increases with deformation. The same assignment was also made by [20] on the basis of calculations with the particle-rotor model.

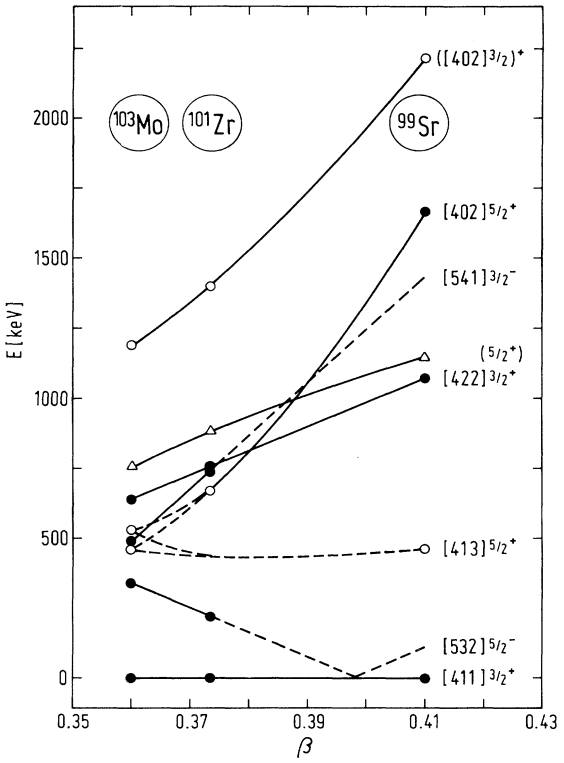

FIG. 7. Systematics of experimental levels with similar decay patterns in the $N = 61$ isotones ^{99}Sr, ^{101}Zr, and ^{103}Mo as a function of quadrupole deformation. Full data points indicate rather well-identified Nilsson configurations. Open points represent more tentative assignments. Open triangles represent the first excited level of the [422]3/2 band. The dashed lines are extrapolations based on the slopes of the single-particle energies vs deformation, as calculated with the Nilsson model.

The 744.0 keV level is proposed to be the head of a band with $K^\pi = 3/2^-$, with the 808.5 keV level being the next band member. In ^{99}Sr, levels with similar γ-decay branches could not be observed but in ^{103}Mo, the level at 489.9 keV obviously corresponds to the 744.0 keV level in ^{101}Zr (Fig. 5). For the 489.9 keV level we derive a logft value of 6.5, which is consistent with odd parity. The only choice for a $K^\pi = 3/2^-$ bandhead is the ν[532]3/2 orbital. Since it is a strongly down-sloping orbital of hole character, its energy should increase by a fairly large amount from ^{103}Mo to the more deformed ^{101}Zr. This is indeed the observed trend. In the $A \simeq 100$ region, so far the [532]3/2 orbital has only been identified in the nucleus $^{97}Sr_{59}$ [21]. The energies of the $K+1 \rightarrow K$ transitions in ^{97}Sr (69.1 keV) and ^{101}Zr (64.5 keV) are similar. The level at 845.3 keV is the possible $7/2^-$ member of the band. Relative to the other band members, its energy is low. Thus, it could be perturbed by the ν[523]7/2 bandhead, which is expected to lie at about this energy.

The levels at 673.5, 786.7, and 902.5 keV could form a band with $K = 3/2$ or 5/2 and probably even parity. The Nilsson scheme shows that low-lying odd-parity orbitals with $K = 3/2$ and 5/2 have been exhausted, so that even parity is, indeed, a reasonable choice. The only still available low-lying levels of even parity have both $K = 5/2$, namely the ν[413]5/2 and the ν[402]5/2 orbitals. There are states in the $N = 61$ neighbors with a decay pattern quite similar to the one of the 673.5 keV level. These are the level at 422.5 keV in ^{99}Sr and both states at 456.1 and 526.1 keV in ^{103}Mo (Fig. 5). The 422.5 keV level in ^{99}Sr is clearly a good candidate for a $5/2^+$ state. It may form a band with the 535.0 keV level and its logft value of 5.9 indicates an allowed transition from the $3/2^+$ ^{99}Rb ground state [37,38]. In ^{103}Mo, both levels at 456.1 and 526.1 keV have a decay pattern fairly similar to that of the Sr level. Accordingly, the level at 422.5 keV in ^{99}Sr and one of the ^{103}Mo levels at 456.1 or 526.1 keV could be associated with the [413]5/2 orbital, since this $5/2^+$ orbital keeps parallel to the [411]3/2 ground-state orbital in the deformation range $\beta = 0.3 - 0.4$. In ^{101}Zr a level at this energy is not identified. Consequenly, the higher-lying 673.5 keV level and the second one of the above-mentioned ^{103}Mo levels could be associated with the other $5/2^+$ bandhead, namely the [402]5/2 orbital of particle character, which is strongly up-sloping, in agreement with the observed trend of excitation energies. An extrapolation of the trend to ^{99}Sr makes the level at 1669.5 keV the best candidate for the [402]5/2 orbital. Finally we note that in ^{101}Zr, the [402]5/2$^+$ bandhead is close to the $5/2^+$ level ($I = K + 1$) from the [422]3/2 band (Fig. 6). The repulsive interaction, pushing upwards the 5/2 level of the [422]3/2 band, could account for the energies of the $K+1 \rightarrow K$ transitions in the $K = 3/2$ band, somewhat larger in ^{101}Zr (120.9 keV) than in ^{103}Mo (105.1 keV).

As discussed in [13], the strongly up-sloping hole $\nu[404]9/2$ orbital seems to play an important role in stabilizing the deformation of the Sr isotopes near $N = 60$ by compensating the deformation-driving force of the down-sloping particle [532]5/2 orbital. The [404]9/2 orbital was postulated by Meyer *et al.* [41] to correspond to an isomer observed in former prompt-fission experiments [42]. In that work γ lines at 91.6, 98.2, and 133.7 keV were assigned to the ^{101}Zr scheme and they showed a delay of $\simeq$ 18 ns with respect to fission. These data suggest the existence of an isomer at 323.5 keV, decaying to the $7/2^+$ level at 231.9 keV (of the $K = 3/2$ ground-state band) through the 91.6 keV transition. In the present work, we noted that the intensities of both lines depopulating the $7/2^+$ level are somewhat higher than were measured in previous experiments at JOSEF [17]. This observation might have indicated an additional feeding through this postulated $9/2^+$ isomer. However, our β-γ-t coincidence data neither show evidence for the above 91.6 keV line, nor for a 18 ns delay of the 98.2 and 133.7 keV transitions. From this we conclude that the $9/2^+$ isomer discussed by [41] is not populated in β decay of ^{101}Y. In ^{103}Mo, the [404]9/2 orbital was proposed to correspond to the 353.8 keV level [31], but in the mean time, this assignment was found to be incorrect [20]. Thus, neither in ^{101}Zr nor in ^{103}Mo, the [409]9/2 orbital has been identified among the excited states. In ^{99}Sr, the strongly up-sloping [404]9/2 hole orbital is expected at very low energy. The observation of levels with spins up to $I^\pi = 11/2^+$ in the β decay of ^{99}Sr ($I^\pi = 3/2^+$) to ^{99}Y [38–40] might indicate the β decay of a, so far nonidentified, high-spin isomer in ^{99}Sr, which could correspond to the [404]9/2 orbital. This would set a rather restrictive upper limit on its excitation energy, since if it were lying well above the first excited state ($I^\pi = 5/2^+$) at 90.8 keV, it could decay via an $E2$ γ transition with a moderate K-hindrance factor.

Finally, among the high-energy levels the 2320.6 (^{99}Sr), 1398.6 (^{101}Zr), and 1185.6 keV (^{103}Mo) levels all have a strong branch to the $5/2^+$ state. If they have the same nature, the trend of their excitation energies is consistent with their assignment to the [402]3/2 orbital.

In summary, all ^{101}Zr levels at low energy have been associated either to Nilsson neutron orbitals or to the lowest band members built on them. Conversely, the expected low-lying Nilsson orbitals except the [411]1/2 and [404]9/2 orbitals, have been associated with experimental levels, at least in two of the ^{99}Sr, ^{101}Zr, or ^{103}Mo isotones. The existence of the decoupling parameter for $K = 1/2$ bands makes our simple arguments based on energy spacings within the band members impossible, although some members might be populated in the decay from the $I^\pi = 5/2^+$ mother nucleus ^{101}Y. On the contrary, population of the $K = 9/2$ band has to be weak and this explains why the [404]9/2 orbital has not been identified so far in this region.

C. Particle-rotor model calculations

A calculation of the levels in ^{103}Mo was recently performed [20] in the frame of the particle-rotor coupling model, using parameters ($\kappa_n = 0.084$, $\mu_n = 0.28$) optimized for this nucleus. Given its success, the calculation was repeated for ^{101}Zr and ^{99}Sr with the same parameter set but for different deformations. In this calculation the Coriolis mixing is a crucial ingredient in order to account for the perturbation of energies and transition probabilities in the low Ω bands of $h_{11/2}$ origin. This was especially well demonstrated in the prompt fission studies by Hotchkis *et al.* [16], who have observed the $5/2^-$ band up to at least $I = 15/2$ in ^{101}Zr, ^{103}Mo, and ^{103}Zr.

For ^{101}Zr the best agreement with the experiment was achieved at the deformation of $\beta = 0.36$ (see Fig. 6), which is also the value adopted from lifetime measurements and level systematics. In addition to the [411]3/2 ground-state band, also the excited rotational bands are reasonably well reproduced. The $\nu[422]3/2^+$ bandhead is calculated at about 660 keV; this is to be compared to the experimental level at 759 keV. The odd-parity band head $\nu[532]5/2$ is predicted at 142 keV, fairly close to the experimental energy of 217 keV. The [404]9/2 orbital, discussed in [41], is calculated below the $7/2^+$ member of the ground-state band.

For ^{99}Sr the agreement is less satisfactory at the measured deformation of $\beta = 0.40$. The [422]3/2 orbital is about 400 keV too low. In order to shift it up to the experimental energy of 1071 keV, an even stronger deformation of $\beta = 0.44$ has to be chosen. This value is still consistent with the experimental deformation. However, the [404]9/2 orbital becomes the ground state, 230 keV below the [411]3/2 bandhead. This situation cannot be excluded by our present knowledge of the decay scheme of ^{99}Sr, but, as already mentioned, there is so far no direct evidence for such a level.

VI. CONCLUSION

This study has considerably extended the level scheme of ^{101}Zr. This nuclide is the first odd-neutron Zr isotope in the deformed $A \simeq 100$ region and represents the missing link between the $N = 61$ isotones ^{99}Sr and ^{103}Mo for which detailed level schemes and values of the deformation were available. The previously known [411]3/2 ground-state band has been confirmed. The band built on the 216.7 keV level has been firmly identified as $K^\pi = 5/2^-$, and can be associated with the [532]5/2 Nilsson orbital. For the first time, K-conversion coefficients for the $K+1 \rightarrow K$ transitions in both bands have been measured. Lifetimes of the first excited members of both bands have been determined and confirm the existence of strong deformation in the range $\beta \simeq 0.3 - 0.4$. In addition, a number of rotational levels are identified on the basis of level systematics of the $N = 61$ isotones ^{99}Sr, ^{101}Zr, and ^{103}Mo. Below an excitation energy of about 1 MeV, all experimental levels in ^{101}Zr are associated either with Nilsson orbitals or with corresponding band members. The level schemes of ^{101}Zr and ^{103}Mo turn out to be very similar. In contrast, the level scheme of ^{99}Sr clearly reflects the changes induced by higher deformation. The trends of excitation energy for levels with similar γ-ray decay patterns establish that ^{101}Zr is only slightly more

strongly deformed than ^{103}Mo. The quadrupole deformation parameter is estimated to $\beta = 0.37(2)$. The proposed interpretation of the rotational structure of ^{101}Zr is supported by calculations with the particle-rotor model.

Summarizing, although both Sr and Zr isotopes show an unusually rapid lowering of the deformed minimum of the potential-energy surface, known as the *sudden onset of deformation*, the evolution of the magnitude of deformation is smoother in Zr and resembles rather the one in the, somewhat less deformed, Mo neighbor nuclei. Thus, the unique feature of a saturation of deformation at its onset observed in the Sr isotopes cannot be accounted for exclusively in terms of the occupancies of valence neutron orbitals but, probably, reflects the influence of the strong $Z = 38$ deformed gap and of the change in the integrated proton-neutron interaction.

As a final remark, the position of the [404]9/2 orbital is very sensitive to the deformation and to the spin-orbit splitting. Lifetime measurements could be a tool for the identification of this orbital in the moderately deformed nuclei, owing to the K hindrance for the decay into the ground-state band. For strongly deformed nuclei, where this orbital is to be lying very low, a search for isomeric decay by electron spectroscopy could be rewarding.

ACKNOWLEDGMENTS

This work was supported by the German Federal Minister for Research and Technology (BMFT) under Contract No. 06 MZ 106.

[1] *Table of Isotopes*, 7th ed., edited by C. M. Lederer and V. S. Shirley (Wiley, New York, 1978).

[2] See, for instance, contributions by G. Molnár *et al.*, in *Proceedings of International Workshop on Nuclear Structure of the Zr Region*, edited by J. Eberth, R. A. Meyer, and K. Sistemich, Springer Reports on Physics (Springer-Verlag, Berlin, 1988).

[3] OSTIS and ISOLDE Collaborations, G. Lhersonneau, K.-L. Kratz, J. Äystö, H. Gabelmann, J. Kantele, B. Pfeiffer, *Proceedings of the Sixth International Conference on Nuclei far from Stability and the Ninth International Conference on Atomic Masses and Fundamental Constants*, edited by R. Neugart and A. Wöhr Institute of Physics Conference Series No. 132 (IPP, Bristol, 1992), p. 545.

[4] ISOLDE Collaboration, G. Lhersonneau, B. Pfeiffer, K.-L. Kratz, T. Enqvist, P. P. Jauho, A. Jokinen, J. Kantele, M. Leino, J. M. Parmonen, H. Penttliä, and J. Äystö, Phys. Rev. C **49**, 1379 (1994).

[5] H. Ohm, M. Liang, G. Molnar, and K. Sistemich, Z. Phys. A **334**, 519 (1989).

[6] H. Mach, M. Moszynski, R. L. Gill, F. K. Wohn, J. A. Winger, J. C. Hill, G. Molnar, and K. Sistemich, Phys. Lett. B **230**, 21 (1989).

[7] H. Ohm, M. Liang, G. Molnár, and K. Sistemich, Z. Phys. A **334**, 519 (1989).

[8] J. C. Hill, D. D. Schwellenbach, F. K. Wohn, J. A. Winger, R. L. Gill, H. Ohm, and K. Sistemich, Phys. Rev. C **43**, 2591 (1991).

[9] R. C. Jared, H. Nifenecker, and S. G. Thompson, *Proceedings of the Third Symposium on Physics and Chemistry of Fission,* IAEA Rochester, New York (IAEA-SM-174 Vienna, 1974), p. 211

[10] H. Mach, F. K. Wohn, M. Moshzynski, R. L. Gill, and R. F. Casten, Phys. Rev. C **41**, 1141 (1990).

[11] H. Mach, M. Moszynski, R. L. Gill, G. Molnár, F. K. Wohn, J. A. Winger, and J. C. Hill, Phys. Rev. C **41**, 350 (1990).

[12] F. K. Wohn, H. Mach, M. Moszynski, R. L. Gill, and R. F. Casten, Nucl. Phys. **507**, 141c (1990).

[13] ISOLDE Collaboration, G. Lhersonneau, H. Gabelmann, N. Kaffrell, K.-L. Kratz, B. Pfeiffer, and K. Heyde, Z. Phys. A **337**, 143 (1990).

[14] K. Kawade, G. Lhersonneau, H. Ohm, K. Sistemich, and R. A. Meyer, KFA-Jülich Annual report 1986, p. 21.

[15] F. K. Wohn, J. C. Hill, R. F. Petry, H. Dejbakhsh, Z. Berant, and R. L. Gill, Phys. Rev. Lett. **51**, 873 (1983).

[16] M. C. A. Hotchkis, J. L. Durell, J. B. Fitzgerald, A. S. Mowbray, W. R. Phillips, I. Ahmad, M. P. Carpenter, R. V. F. Janssens, T. L.Khoo, E. F. Moore, L. R. Morss, Ph. Benet, and D. Ye, Nucl. Phys. A **530**, 111 (1991).

[17] H. Ohm, G. Lhersonneau, U. Paffrath, K. Shizuma, and K. Sistemich, Z. Phys. A **326**, 233 (1987).

[18] ISOLDE Collaboration, G. Lhersonneau, H. Gabelmann, N. Kaffrell, K.-L. Kratz, and B. Pfeiffer, Z. Phys. A **332**, 243 (1989).

[19] ISOLDE Collaboration, P. Lievens, R. E. Silverans, L. Vermeeren, W. Borchers, W. Neu, R. Neugart, K. Wendt, F. Buchinger, and E. Arnold, Phys. Lett. B **256**, 141 (1991).

[20] M. Liang, H. Ohm, I. Ragnarsson, and K. Sistemich, Z. Phys. A **346**, 101 (1993).

[21] G. Lhersonneau, B. Pfeiffer, K.-L. Kratz, H. Ohm, K. Sistemich, S. Brant, and V. Paar, Z. Phys. A **337**, 149 (1990)

[22] G. Lhersonneau, Nucl. Instrum. Methods **157**, 349 (1978).

[23] R. F. Petry, J. D. Goulden, F. K. Wohn, J. C. Hill, R. L. Gill, and A. Piotrowski, Phys. Rev. C **37**, 2704 (1988).

[24] H. Seyfarth, H. H. Guven, B. Kardon, G. Lhersonneau, K. Sistemich, S. Brant, N. Kaffrell, P. Maier-Komor, H. K. Vonach, V. Paar, D. Vorkapic, and R. A. Meyer, Z. Phys. A **339**, 269 (1991).

[25] J. Blachot, Nucl. Data Sheets **45**, 701 (1985).

[26] B. Singh and J. A. Szucs, Nucl. Data Sheets **60**, 1 (1990).

[27] J. Kantele, Nucl. Instrum. Methods Phys. Res. A **275**, 149 (1989).

[28] H. Ohm, M. Liang, U. Paffrath, B. De Sutter, K. Sistemich, A.-M. Schmitt, N. Kaffrell, N. Trautmann, T. Seo, K. Shizuma, G. Molnar, K. Kawade, and R. A. Meyer, Z. Phys. A **340**, 5 (1991).

[29] B. Pfeiffer, K.-L. Kratz, H. Gabelmann, W. Ziegert, V. Harms, and B. Leist, in *Proceedings of Specialists's Meeting on Delayed Neutron Properties*, University of Birm-

ingham, edited by D. R. Weaver (ISBA 07044 0926 7, 1987), p. 75.

[30] M. Gross, P. Jürgens, S. Kluge, M. Mehrtens, S. Müller, F. Münnich, and J. Wulff; *Proceedings of the Sixth International Conference on Nuclei far from Stability and the Ninth International Conference on Atomic Masses and Fundamental Constants*, edited by R. Neugart and A. Wöhr Institute of Physics Conference Series No. 132 (IPP, Bristol, 1992), p. 77.

[31] K. Shizuma, H. Ahrens, J. P. Bocquet, N. Kaffrell, B. D. Kern, H. Lawin, R. A. Meyer, K. Sistemich, G. Tittel, and N. Trautmann, Z. Phys. A **315**, 65 (1984).

[32] OSTIS and ISOLDE Collaborations, G. Lhersonneau, H. Gabelmann, B. Pfeiffer, and K.-L. Kratz, in *Proceedings of the First Biennial Workshop on Nuclear Physics*, Megeve France, edited by D. Guinet and J. R. Pizzi (World Scientific, Singapore, 1991), p. 214.

[33] D. De Frenne and E. Jacobs, Nucl. Data Sheets **68**, 935 (1993).

[34] M. Liang, H. Ohm, U. Paffrath, B. De Sutter, and K. Sistemich, KFA-IKP report 1991, p. 16.

[35] R. F. Casten, K. Heyde, and A. Wolf, Phys. Lett. B **208**, 33 (1988).

[36] G. Lhersonneau *et al.*, Z. Phys. A (submitted).

[37] B. Pfeiffer, E. Monnand, J. A. Pinston, J. Münzel, P. Möller, J. Krumlinde, W. Ziegert, and K.-L. Kratz, Z. Phys. A **317**, 123 (1984).

[38] H.-W. Müller and D. Chmielewska, Nucl. Data Sheets **48**, 663 (1986).

[39] R. F. Petry, H. Dejakhsh, J. C. Hill, F. K. Wohn, M. Schmid, and R. L. Gill, Phys. Rev. C **31**, 621 (1985).

[40] F. K. Wohn, Phys. Rev. C **36**, 1204 (1987).

[41] R. A. Meyer, N. Kaffrell, H. Lawin, G. Lhersonneau, E. Monnand, V. Paar, B. Pfeiffer, J. A. Pinston, I. Ragnarsson, F. Schussler, A. Schmitt, T. Seo, K. Sistemich, and N. Trautmann, Proceedings of NEANDC Specialists Meeting on Yields and Decay Data of Fission Product Nuclei, edited by R. E. Chrien and T. W. Burrows (Brookhaven National Laboratory, Report BNL51778, 1983), p. 321.

[42] R. G. Clark, L. E. Glendenin, and W. L. Talbert, Jr., in [9], p. 221.